



# The optimization of nodes clustering and multi-hop routing protocol using hierarchical chimp optimization for sustainable energy efficient underwater wireless sensor networks

Shukun He<sup>1</sup> · Qinlin Li<sup>2,3</sup> · Mohammad Khishe<sup>4</sup> · Amin Salih Mohammed<sup>5,6</sup> · Hassan Mohammadi<sup>4</sup> · Mokhtar Mohammadi<sup>7</sup>

Accepted: 13 June 2023

© The Author(s), under exclusive licence to Springer Science+Business Media, LLC, part of Springer Nature 2023

## Abstract

The design of underwater wireless sensor networks (UWSNs) faces many challenges, including power consumption, storage, battery life, and transmission bandwidth. UWSNs usually either use node clustering or multi-hop routing as their energy-efficient optimization algorithms. The cluster optimization technique will organize the sensor nodes into a cluster network, with each cluster led by a cluster head (CH). In contrast, the multi-hop optimization algorithm will create a multi-hop network by sending data to the base station (BS) while switching between different sensor nodes. However, the overburdens of CH nodes impact the performance of the cluster optimization method, whereas the overburdens of nodes close to the BS impact the performance of the multi-hop optimization algorithm. Therefore, clustering and routing procedures can be considered as a simultaneous NP-hard problem that metaheuristic algorithms can address. With this motivation, this paper proposes an energy-efficient clustering and multi-hop routing protocol using the metaheuristic-based algorithm to increase energy efficiency in UWSNs and lengthen the network life. However, the existing metaheuristic-based methods use two separate algorithms for clustering and multi-hop routing, increasing computational complexity, different initialization, and difficulty in hyperparameters' tuning. In order to address the mentioned shortcomings, this paper proposes a novel hierarchical structure called hierarchical chimp optimization (HChOA) for both clustering and multi-hop routing processes. The proposed HChOA is validated using various metrics after being simulated using an extended set of experiments. Results are compared to those from LEACH, TEEN, MPSO, PSO, and IPSO-GWO to validate the impact of the HChOA. According to the findings, the HChOA performed better than other lifespan and energy usage benchmarks.

**Keywords** Nodes clustering · Multi-hop routing · Chimp optimization algorithm · Hierarchical

## 1 Introduction

Underwater wireless sensor networks (UWSNs) have numerous independent, homogenous probes with a restricted-energy supply [1]. These underwater probes are installed in seas and oceans to measure the temperature [2], pressure [3], current flow [4], and water quality in the water environment [5]. Data processing stations collect this information according to specific applications [6]. Humans can use numerous applications, including ambient monitoring [7], event predictions [8, 9], medical and biological problems [10, 11], military detection [12], radar and

LIDAR [13, 14], social network [15, 16], nonstationary systems [17], decision-making systems [18–20], and spammer detector [21], by observing their surroundings [22, 23].

The UWSN [24] is made up of sink nodes, onshore BSs, and underwater probes [25, 26]. The remaining nodes formed clusters, while the submerged nodes were located near the sink sensor node [27]. The surface sink node receives data from the underwater probes via communication. The information collected by the sink node is subsequently transmitted to the closest BS located on the coastline [28]. In UWSNs, there is an acoustic transducer that allows for inter-node communication. Also, the sink node contains a transmitter and receiver that establishes a

Extended author information available on the last page of the article

radio frequency (RF) link to the BS. Channel modeling [29], path loss [30], uncertainty [31], self-recoverability [32], privacy [33, 34], security [35], reliability [36, 37], stabilization level [38], robustness [39], amplitude imbalancing [40], and network structure [41] are all different in an underwater setting compared to a terrestrial wireless sensor network (TWSN) [42].

TWSNs and UWSNs transfer data packets from a sensor to a BS through a one-hop or multi-hop connection. [43]. The packet of data must be transmitted from one node to another without being corrupted [44]. Since each node has its own battery, which might be challenging to recharge or replace, retransmitting data packets can significantly drain the power. This could result in a rapidly degrading network or a high proportion of nodes failing prematurely [45].

The majority of current methods have concentrated on using either multi-hop routing or node clustering as their energy-efficient optimization algorithms [46]. However, the performance of the cluster optimization technique is affected by the overburdens of CH nodes, whereas the performance of the multi-hop optimization approach is affected by the overburdens of nodes adjacent to the BS [47]. This means that clustering and routing processes are joint NP-hard problems that can be solved with metaheuristics [48, 49]. The main goal of such an optimization technique is to enhance UWSN energy efficiency while enhancing the overall performance of the network lifetime over a given area [50]. In order to improve energy efficiency in UWSNs and extend the life of the network, this research offers an energy-efficient clustering and multi-hop routing protocol utilizing a metaheuristic-based algorithm (i.e., HChOA).

## 1.1 Related works and motivation

Numerous clustering protocols have been developed for TWSNs to minimize sensor energy consumption while reliably sending data packets. Previous research studies are generally divided into two main categories: (1) conventional approaches and (2) metaheuristic-based approaches. In the following, several main and influential references from each group are reviewed, and their advantages and disadvantages are highlighted.

### 1.1.1 Conventional approaches

TWSNs have homogeneous, energy-limited nodes. A low-energy adaptive clustering hierarchy (LEACH) successfully reduces node energy consumption as a consequence, maintaining network lifetime [51]. Since each CH's acoustic range is limited, connections between each CH and the sink node in the LEACH protocol may fail in large-scale sensor node deployment. Additionally, single-hop

communication may greatly increase traffic at the sink node, and collisions will frequently happen in networks.

Reference [52] examined a clustering protocol for UWSNs, proving suitable for underwater transmission. Reduced overall power consumption, longer node lifetimes, and improved network resilience are all benefits of this method's clustering protocol's architecture. Nevertheless, the cluster must maintain network communication to guarantee full coverage, which is difficult given the probe's current state. With a novel routing protocol described in [53], nodes can self-organize into groups with similar energy and connectivity levels. This model computes the best route based on signal strength and average energy. The mechanism used by this protocol to choose header nodes ignores both the CH's lifetime and the nodes' locations [45]. Because of the increased heat generated by the CH, a sensor node may be destroyed if it acts as CH for too long.

In this method, the clustering protocol is made to minimize control information, which reduces overall energy usage, lengthens node lifespan, and boosts model resilience. In order to ensure total coverage, the cluster must maintain network communication given the current impact on the probe. According to their energy and depth, nodes in [53] can group into clusters due to a special routing protocol. Based on signal quality and remaining energy, this model selects the ideal routing path. The lifetime of the CH or the location of the nodes is not taken into account by this protocol's mechanism for choosing header sensors. A hot spot may develop if a node acts as the CH for a prolonged period of time, eliminating the sensor node.

A UWSN cluster was constructed in [53] using LEACH. The research also evolved LEACH by administering controlled LEACH. The control nodes run the clustering protocol while the controlling probe is placed in the center of the network's component by the controlled-LEACH, giving the network a longer lifespan than the classical LEACH. Due to the necessity of communication between sensor nodes and the controlling nodes, this method takes a while to complete the clustering procedure.

The CHs are allocated randomly due to the inability of LEACH and controlled-LEACH to apply a knowledge CH-choosing mechanism, which increases energy consumption. Therefore, it is suggested to build primarily balanced clusters using the base-station-controlled dynamic clustering protocol (BCDCP) [54]. BCDCP eliminates duplicate CHs by having an equal component for each of them and by sending data to the BS through CH routing. In order to lengthen the lifespan of nodes and reduce the price of data transfer among them, researchers are developing a few position-aware protocols.

A research study [55] developed an adaptive clustering-routing algorithm for UWSNs using an optimization

technique. Retransmissions can cause data packets to be doubled or the recipient to experience longer delays due to cluster member selection. The MLCEE protocol, described in [56], aims to increase network lifespan, thereby minimizing packet delay. Since there are many levels in the network, each node can play the role of a forwarder based on its probability and energy. The TCEB protocol was implemented according to reference [57] to balance system lifetime and energy consumption in the intended UWSN. A multi-hop routing mechanism was implemented in [58] using a different clustering protocol approach. By using this technique, probes can modify their energy usage while obtaining the greatest UWSN performance. Attaching a probe to neighboring nodes is required for this use of the optimized power clustering method.

An energy-balanced asymmetric multilayer clustering algorithm was developed for UWSNs to minimize energy usage throughout inter-cluster communications. This method generates clusters of varying sizes within the same layer in order to address the “hot spot” issue [59]. The next-hop CH selected by the node is the one with the minimum fitness function value.

Reference [60] presented a clustered geographic-opportunistic routing system for UWSNs. They suggested two techniques in this work: cluster formation algorithms and beacon algorithms. All sensor nodes’ locations are found using the beacon technique. Then, the cluster creation algorithm is used to choose and elect CHs from among the normal nodes in a group. The only factor used to distinguish CHs from regular nodes is distance. This work has no procedure for dealing with unexpected circumstances like CH failure.

Reference [61] developed the MPODF protocol based on mobility prediction for UWSNs. The MPODF source routing protocol predicts an energy-efficient approach to the sink. The MPODF protocol uses the computed temporal locations of every sensor provided by the mobility model to determine the best route to the sink at the source node level. The MPODF protocol can determine a single optimum path to the sink without utilizing any localization approaches based on the mobility model for sensor node networks that are freely floating. It helps the protocol pick a potential forwarder on the most efficient route to the sink. Even though this protocol eradicates the localization problem, the issue with this protocol is failure handling in the case of forwarder node failure [62].

In research [63], the authors propose a secure routing algorithm for underwater (SRAU) sensor networks to avoid wormhole and Sybil attacks. This algorithm consists of four stages. In underwater acoustic networks, the initial step is to safely find neighbors despite wormhole attacks. Stage two is the significant route discovery process, which finds the next dependable sink node transmitting node,

improving the chance of packet delivery to the sink and boosting reliability. The method of detecting an attack during data distribution is the third stage. The Sybil attack can be detected in this stage using information about the state of nodes. Finding an alternate, safe path to detect rogue nodes is the fourth stage in the process. In this algorithm, the issue is packet transmission overhead, which reduces the network lifetime, and there is no cluster formation. All the nodes participate in the routing process, which is an overhead for the network.

In research [64], the author proposed a bi-objective routing protocol for UWSNs. Planned routes are optimized for delay and dependability using a modified best search and an uninformed search technique. An uninformed search technique finds routes from each sensor node to a particular surface sink with information on the entire topology but without any information about the delay or dependability on individual links. The nodes are selectively expanded based on their dominance to reduce the computational time complexity. The issue with this protocol is applicable as two alternate heuristic methods are proposed using the greedy bi-objective routes selection function. In [65], the authors proposed a two-stage routing protocol to enable the connected and partitioned nodes to report their data successfully. Beacons are used to transmit neighborhood information throughout the network in phase one. Here, an approach to reach and spread information about the neighborhood to the network’s disconnected components is developed as phase 1. Phase 2 involves selecting appropriate relay nodes for sending the collected data to the sink node using the neighborhood information gathered in phase 1. In order to keep busy nodes from dying prematurely, a minimal residual energy threshold strategy is utilized. When one of the relay nodes can no longer function as a relay due to a lack of residual energy, it creates a rerouting mechanism to route the track. In this work, there is a failure handling mechanism, but it did not consider the overhead at the forwarding node, which will reduce the network’s performance.

### 1.1.2 Metaheuristic approaches

A gravitational search algorithm was proposed in reference [66] for locating the best CHs among the nodes. The node’s remaining energy was taken into account when selecting the CH. Energy efficiency, intra-cluster distance, and distance to BS were the fitness functions taken into account when choosing the CH. In order to get data from the sensor node to CH, a single-hop solution was used. The next hop was chosen using a multi-hop technique based on the fitness function to transport the data across WSN. The only factors taken into account by the fitness function of the

multiple-hop technique are the next hop's residual energy and its range from the BS.

In the reference [67], a harmony search algorithm was provided to cluster the network in the WSN. The clustering fitness functions include the node degree, energy, intra-cluster distance, and CH-BS distance. By choosing the node with the shortest transmission distance, the node's energy usage was decreased. The network performance is impacted when clusters have a significant number of non-CH members.

In the reference [68], a biogeography-based optimization (BBO) was provided to choose CH from the network by taking fitness function values, such as distance between cluster nodes, the distance between CHs and the BS, and residual energy, into account. Actually, the BBO generated the shortest route between CH and BS. By keeping the remaining sensors' remaining energy, BS could receive the most data packets. When the BS was outside the network, the network's remaining energy was marginally diminished compared to genetic algorithm-based routing.

In reference [69], optics-inspired optimization (OIO) was suggested for WSN clustering and routing. Node degree, energy, and distance were three distinct characteristics used in clustering and routing optimization to produce the best clusters and transmission paths. The OIO chose the CH initially during the clustering process, and then a potential fitness function was started to allocate the nodes to the chosen CH. In order to prevent packet loss in the network, a node with more energy was chosen as the next hop (i.e., CH). The computational complexity of OIO-based clustering and routing rises exponentially with network size despite employing the same method for both tasks.

The hybrid particle swarm optimization and simulated annealing-based polynomial time clustering methods in WSN were developed by reference [70]. There were two setup and steady-state phases for these clustering techniques. During the cluster setup step, the CH was chosen, and the cluster was formed. Normal nodes have their modes set to sleep until they are used for data transmission. The normal nodes then sent the data to the appropriate CH during their particular time division multiple access time slot. Additionally, CH transfers the data packets it receives from its regular nodes to the BS.

In order to obtain an unbalanced cluster in WSN, reference [70] provided the chemical reaction optimization (CRO). In order to choose the CHs according to the median sink distance, energy ratio, and node distance, the CRO was combined with a possible energy function and molecular encoding structure. Next, depending on the cost function, the regular sensor nodes were assigned to the desired CHs. By choosing the best CHs from the network, the imbalanced energy usage was minimized using this

technique. This CRO-based clustering and routing method does not take fault tolerance into account.

According to reference [71], the EMEER protocol was created for WSN. The cuckoo search method clustered the network in the EMEER protocol based on similarity and energy-level criteria. Then CH was chosen based on the trust value, energy, and range from the nodes to sink. The network used less energy than the conventional algorithms LEACH, PEGASIS, and TEEN protocols. This EMEER protocol does not evaluate the performance of the living nodes during communication.

In order to improve the network's energy efficiency, reference [72] presented the ant-lion optimization (ALO) approach for clustering. The ALO's fitness function takes the residual energy, the number of nearby nodes, the distance between the nodes, and the range between the BS and the node. The node with the highest level of fitness was regarded as the CH. Then, using a discrete ALO technique, the best route linking the CHs and the BS was discovered.

In order to reduce the energy usage of the WSN, reference [73] developed PSO-based energy-limited clustering routing. The sensor node with the highest residual energy was deemed a candidate CH during the clustering procedure. Data transmission between the nodes and the CH and between the CH and the BS started after the comprehensive PSO clustering. An additional amount of energy was needed in the WSN for the data collecting, aggregation, and distribution of CH.

The fractional lion (FL) clustering technique was created by reference [74] to produce the best possible routing path in the WSN. The FL algorithm's fitness function took five criteria into account: delay, the energy of CH and regular nodes, and intra-cluster and inter-cluster distance. The FL algorithm found the neighbor solution by using fractional order derivatives. Next, the network lifetime was increased by utilizing the FL algorithm's efficient CH selection. The node degree is not taken into account throughout the clustering process by this FL clustering algorithm.

Reference [75] proposed a metaheuristic-based energy-efficient clustering with the multi-hop routing protocol. **In this research**, the authors combined the grey wolf optimizer and improved particle swarm optimizer to optimize the clustering and routing processes. **Although** this combined method surpassed the above-mentioned methods, it suffers from **high computational complexity** due to sequentially utilizing two metaheuristic algorithms. UWSNs usually use node clustering or multi-hop routing as their energy-efficient optimization algorithms. However, the overburdens of CH nodes impact the performance of the cluster optimization method, whereas the overburdens of nodes close to the BS impact the performance of the multi-hop optimization algorithm. Therefore, clustering and routing

procedures can be considered as a simultaneous NP-hard problem that metaheuristic algorithms can address [76]. With this motivation, this paper proposes an energy-efficient clustering and multi-hop routing protocol using the metaheuristic-based algorithm to increase energy efficiency in UWSNs and lengthen the network life.

Our motivations for choosing ChOA among other exciting metaheuristic algorithms are as follows:

- **No free lunch theorem** [77]: this theorem states that no metaheuristic optimization algorithm can solve all optimization problems. The only way to find out the capability of an optimization algorithm to solve an optimization problem is to apply that particular optimization algorithm to that particular problem [18].
- **The merit of ChOA**: the ChOA has successfully applied to various optimization problems in a wide variety of fields of study, including sonar and radar target classification [78–80], COVID-19 diagnosis [81], multilevel thresholding segmentation [82], binary optimization problems [83], multimodal and multidimensional optimization problems [84–89], Parkinson's disease diagnosis [90], Solar photovoltaic model parameter identification [91], marine mammal classification [92], and Optimization of constraint engineering problems [88].

## 1.2 Challenges and contributions

Generally, the existing metaheuristic-based methods use two separate algorithms for clustering and multi-hop routing, increasing computational complexity, different initialization, and difficulty in hyperparameters' tuning. This paper provides a novel hierarchical structure called **hierarchical chimp optimization (HChOA)** for both clustering and multi-hop routing processes to solve the above-mentioned problems.

The following list summarizes this study's significant contributions:

- When choosing the CH, the WSN uses the ChOA because of its outstanding stability and low processing complexity. ChOA chooses the CH in this study based on several objective values.
- The ChOA is used to find the shortest route between CH and BS since it can quickly find solutions in WSN. To get over the constraint of the ambiguous convergence time, the ChOA is optimized in this case with residual energy, distance, and node degree.
- The energy-efficient CH selection and data transmission route generation extend the network's lifespan. Additionally, by reducing the nodes' energy usage while

transferring the data packets, the total number of packets obtained by the BS is enhanced.

The rest of the paper is structured as follows: Sect. 2 represents a brief review of background materials, including ChOA. The proposed methodology and problem formulation are presented in Sect. 3. The experimental results and discussion are presented in Sect. 4. Finally, Sect. 5 shows the conclusion and future study directions.

## 2 Background materials: chimp optimization algorithm (ChOA)

The ChOA is a nature-inspired technique that initially comes from the **natural hunting** behavior of chimpanzees. The **driver, barrier, follower, and assailant** are the four different types of individuals in their community. Although every chimp in a group has a different set of skills, these variations are necessary for accurately depicting the hunting process. The primary mathematical description of ChOA can be modeled as follows:

$$\mathbf{x}_{chimp}^{(t+1)} = \mathbf{x}_{prey}^t - \mathbf{a} \cdot \left| \mathbf{c} \cdot \mathbf{x}_{prey}^t - \mathbf{m} \cdot \mathbf{x}_{chimp}^t \right| \quad (1)$$

where the location vectors for the chimpanzee and the prey are denoted by  $\mathbf{x}_{prey}^t$  and  $\mathbf{x}_{chimp}^t$ , respectively, the current iteration is indicated by  $t$ , and the coefficients  $\mathbf{a}$ ,  $\mathbf{m}$ , and  $\mathbf{c}$  are as follows:

$$\mathbf{a} = 2 \cdot \mathbf{f} \cdot rand_1 - \mathbf{a} \quad (2)$$

$$\mathbf{c} = 2 \cdot rand_2 \quad (3)$$

$$\mathbf{m} = \text{Chaotic\_value} \quad (4)$$

These equations involve a nonlinear decrease in  $\mathbf{f}$  over a range of  $[2.5, 0]$ , random values for  $rand_1$  and  $rand_2$  between 0 and 1, and the  $\mathbf{m}$  vector expressing agents' sexual interest via a set of chaotic vectors [81]. This algorithm starts with the random generation of chimps. Like previous **swarm-based techniques**, this stage requires a starting group of agents to **evolve** continuously across iterations.

The four aforementioned categories of agents are assigned randomly. All groups will make an effort to estimate the **best prey locations, but every chimp's model will specify how the positions of the chimps are altered by identifying the  $\mathbf{f}$  vector**. The optimal position is the one assumed by the prey. Iterative adjustments to the  $\mathbf{c}$  and  $\mathbf{m}$  vectors help the system avoid local minima and speed up convergence.

Some examined  $\mathbf{f}$  vectors are summarized in Table 1. The search space can be explored with a wide range of capabilities while keeping exploitation capability



**Table 1** The four dynamic coefficients for **f** vector [93]

Category	<b>f</b> vector
1	$1.95 - 2 \times t^{1/4}/T^{1/3}$
2	$1.85 - 3 \times t^{1/3}/T^{1/4}$
3	$(-3 \times t^3/T^3) + 1.5$
4	$(-2 \times t^3/T^3) + 1.5$

thanks to a variety of dynamic approaches for updating **f** in separate categories.

Although the assailant chimp typically takes charge of the exploitation phase, the other chimps may join in the hunting phase occasionally. Mathematical simulations of the hunting process are used because it is impossible to identify the prey's ideal position in advance. The best agents are the initial driver, assailant, follower, and barrier chimps, while the other agents change their positions accordingly. The location updating rule is represented by the equations below:

$$\begin{aligned} \mathbf{x}_1 &= \mathbf{x}_{Attacker}^t - \mathbf{a}_1 |\mathbf{c}_1 \mathbf{x}_{Attacker}^t - \mathbf{m}_1 \mathbf{x}^t| \\ \mathbf{x}_2 &= \mathbf{x}_{Barrier}^t - \mathbf{a}_2 |\mathbf{c}_2 \mathbf{x}_{Barrier}^t - \mathbf{m}_2 \mathbf{x}^t| \end{aligned} \quad (5)$$

$$\begin{aligned} \mathbf{x}_3 &= \mathbf{x}_{Chaser}^t - \mathbf{a}_3 |\mathbf{c}_3 \mathbf{x}_{Chaser}^t - \mathbf{m}_3 \mathbf{x}^t| \\ \mathbf{x}_4 &= \mathbf{x}_{Driver}^t - \mathbf{a}_4 |\mathbf{c}_4 \mathbf{x}_{Driver}^t - \mathbf{m}_4 \mathbf{x}^t| \end{aligned}$$

$$\mathbf{x}(t+1) = \frac{\mathbf{x}_1 + \mathbf{x}_2 + \mathbf{x}_3 + \mathbf{x}_4}{4} \quad (6)$$

Chaotic maps have been proven to speed up convergence and prevent local optima from being trapped in challenging high-dimensional problems. Table 2 demonstrates the use of four chaotic systems embedded within predictable equations with random characteristics. Assume that half of the individuals can function regularly and the other half can use chaotic methods to determine their following location. The theoretical definition of this method's updating formula is Eq. (7):

$$\mathbf{x}_{chimp}^{(t+1)} = \begin{cases} \mathbf{x}_{prey}^t - \mathbf{a} \cdot \mathbf{d} & \text{if } \mu < 0.5 \\ \text{Chaotic\_value} & \text{if } \mu \geq 0.5 \end{cases} \quad (7)$$

**Table 2** Chaotic maps

No	Name	Chaotic map	Range
1	Sine	$x_{i+1} = \sin(\pi \times x_i)$	(0, 1)
2	Gauss/mouse	$x_{i+1} = \begin{cases} 1 & x_i = 0 \\ \frac{1}{\text{mod}(x_i, 1)} & \text{otherwise} \end{cases}$	(0, 1)
3	Bernoulli	$x_{i+1} = 2 \times x_i \pmod{1}$	(0, 1)
4	Tent	$x_{i+1} = \mu \times (7.7 \times (x_i) - 23.3 \times (x_i^2) + 28.8 \times (x_i^3) - 13.3 \times (x_i^4)), \mu = 1.07$	(0, 1)

where  $\mu$  represents a random number from [0, 1]. Consequently, ChOA is initially started by creating random individuals. Next, each individual is assigned to one of the previously mentioned four independent groups. The agents then use the provided classified approach to update their **f** vector. Furthermore, the four groups assess the potential prey locations during iterations. Then, the distances between the agents and the prey can be updated. Finally, chaotic maps expedite the convergence rate while avoiding local minima stagnation.

### 3 Proposed methodology and problem formulation

The proposed HChOA algorithm consists of two stages: clustering based on **chimp1** and routing based on **chimp2**. An initial step is to set up a sensor field with multiple individual sensors. Once nodes have been placed in the area to be monitored, the BS will send out a beacon signal to individual nodes. Each node will then acquire the sent signal and utilize it to calculate how far it is from the BS.

In order to get to know their surroundings better, the sensors send out “handshaking” signals to any node inside the range. Clustering happens once nearby data have been collected. The **chimp1** method locates the CHs and effectively arranges the clusters. Next, the **chimp2 routing method** is used to find the best routes through the connection. The proposed HChOA optimizes network lifespan and energy usage by combining the benefits of clustering and routing optimization. The whole block diagram of the suggested technique is shown in Fig. 1.

#### 3.1 Network model

N nodes are typically deployed as part of a UWSN to monitor the underwater environment on a regular basis. As shown in Fig. 2, each sensor component consists of a sensor network, CHs, a BS, a connection module, and a control part. The sensors are evaluated using the following requirements:

- Sensor networks have the ability to switch between a sensing mode, in which they keep tabs on the physical environment, and a communication mode, in which they share information with one another and with the base station. Additionally, they collect data from cluster members;
- The connection of each node manages the data traffic;
- Each sensor node is given an index that corresponds to its location;
- After the disposition, the sensor nodes and BS remain stable;
- All routers and connectors benefit from a higher starting energy;
- All nodes are left uncontrolled after deployment is finished, which may prevent the battery from being able to recharge;
- Physical variables are collected by each sensor node;
- Maintains a transient state and delivers information to the destination node periodically;
- Each node is made up of a collection of transmission energy levels so that sensor nodes are capable of customizing power transmission to the specified recipient's remote nature;
- The connection between nodes is entirely identical; it should be noted that the signal power received determines the distance between sensor nodes.

### 3.2 Lifetime of the network's model

There are numerous methods for defining a UWSN's network lifetime. The network's lifetime is measured in the total number of rounds performed before all the sensors die. Although there is a slight decline in data quality as a result of the first node failure, the operation of the model as a whole is unaffected. When the last network probe expires, the network stops functioning. The first node die (FND), and half node die (HND) are used to examine the UWSNs' lifespan [94].

Even if some network nodes are compromised, the systems may still function normally in other respects. Because of the high concentration of sensor nodes in an area, networks can easily recover from node failures because peers encircle healthy nodes with similar capabilities. Therefore, the FND is just one of several factors taken into account when determining the expected lifetime of a system. Therefore, the effectiveness of using an HND's lifetime to gauge performance at optimum network size. Thus, the network's lifetime is determined by Eq. 8.

$$Ns_P^n = Ns \left[ \gamma = \frac{n}{P} \right] \quad (8)$$

where  $P$  is the overall network's sensor count, and  $n$  represents the number of network nodes. According to

this mathematical model, the p-persistent neighbor discovery (PND) duration is determined by the portion of active nodes falling under a particular threshold level.

### 3.3 Clustering procedure: chimp1

In this procedure, Eq. 9 is used to describe the CH. Note that the non-CH node is denoted by the abbreviation  $\overline{CH}$ .

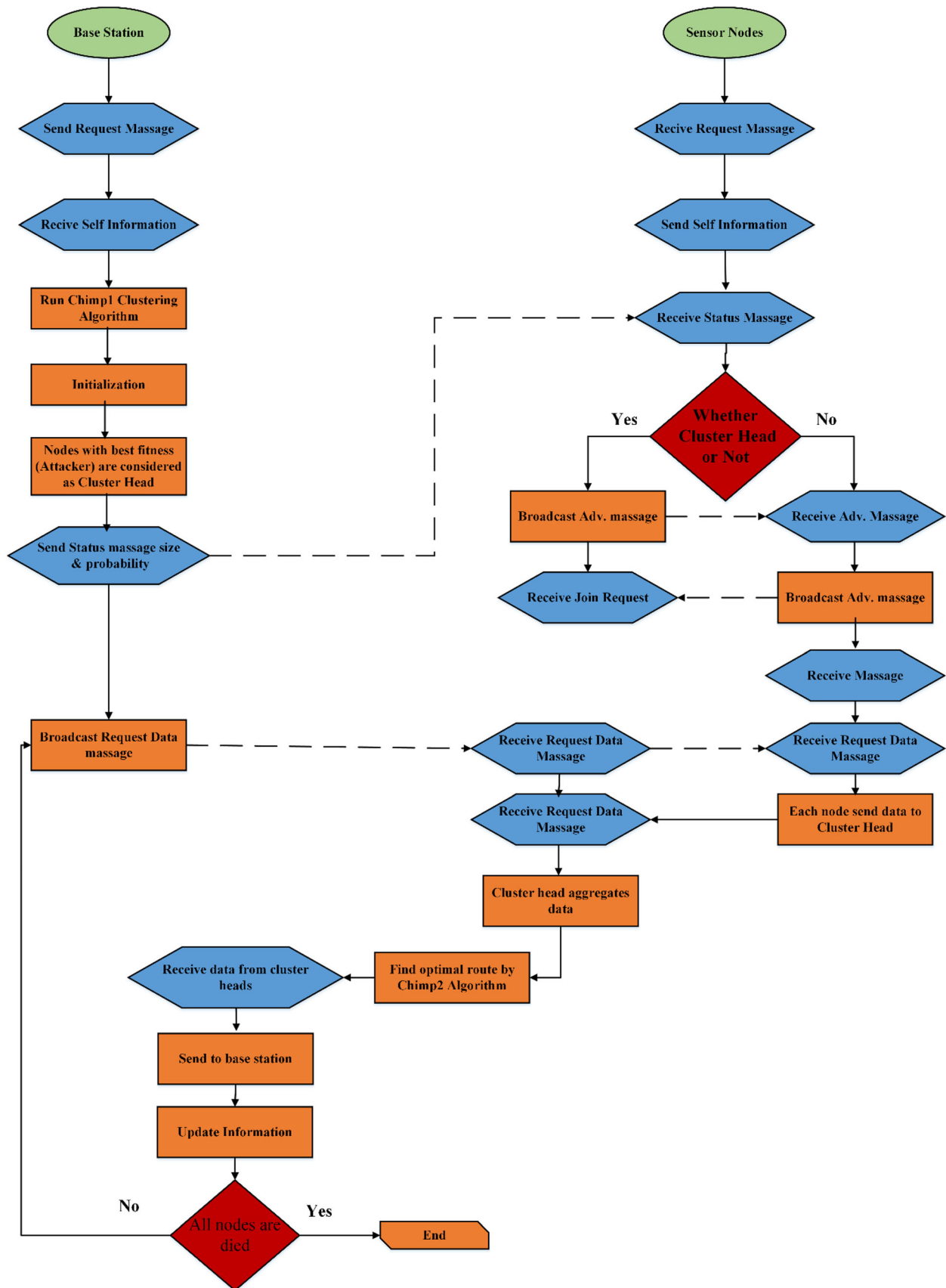
$$CH = \{CH_1, CH_1, CH_1, \dots, CH_{N_c}\} \quad (9)$$

In this method, the CH gathers intra-cluster data, organizes communication among cluster nodes, and connects through relay nodes. When choosing CHs, the energy and position of the nodes are taken into account. The BS will be motivated to form clusters with an even quantity of nodes by selecting CHs with optimum sites and high residual energy. For this, the residual energy of the active nodes in the network is shared with the BS. The BS then finds the clusters with the higher residual energy and maintains the list. For a node to be considered for the CH selection process, the node should have more energy than the threshold energy level. The threshold energy level is defined from time to time based on the network's busy time; for the initial, it will be considered with three fourth of the average energy levels of the active nodes in the network. Once the possible CH nodes list is defined, the BS initiates the CH selection process. Considering the threshold value of the residual energy based on the average residual energy of the active nodes makes the CH selection process optimal as the variable energy levels of the active nodes scenario are subsequently balanced. Consequently, this procedure can be considered an optimization task as formulated in Eq. 10:

$$F_{CH} = \beta \times \frac{\sum_{\forall node_j \in CH} E_{CH}^{residual}(j)/|CH|}{\sum_{\forall node_i \in \overline{CH}} E_{CH}^{residual}(i)/|\overline{CH}|} + (1 - \beta) \times \frac{\sum_{\forall node_i \in CH} d(node_i, base - station)/|\overline{CH}|}{\sum_{\forall node_j \in \overline{CH}} d(node_j, base - station)/|CH|} \quad (10)$$

where,  $d(node_i, base - station)$  denotes the distance connecting node<sub>i</sub> and BS,  $|\overline{CH}|$  and  $|CH|$  signify the non-CH and CH sensors' numbers. This equation is suggested to get the optimal cluster structure and CHs to improve how efficient an average UWSN is at using energy. The predicted lifespan of a node can logically be determined by power output.

The data packet may contain such details. If a node - close to the BS has further residual energy, it is highly feasible to be selected as a CH. This subject is considered an optimization process. Hence, the following subsection





◀Fig. 1 The block diagram of HChOA

utilizes the ChOA approach to optimize the procedure hierarchically.

### 3.4 Routing procedure: chimp2

One entrance and one BS are matched in every outcome. The sizes of the results are comparable across all gateways (Q). In order to assign a random starting number to each node, the approach outlines the route from every node to the BS as follows:

$$G_{p,q} = \text{rand}(0, 1), 1 \leq p \leq N_i, 1 \leq q \leq Q \quad (11)$$

The solution's gateway number is represented by the element q. The gateway  $l_z$  will then be described, along with the path from the BS to the  $l_p$  and which  $l_q$  relays data to  $l_z$ . The map for locating pathways is described in Eq. 12. [75].

$$I_z = \text{Idx}(\text{SetN} \times tL(I_q), \text{Ceil}(G_{p,q} \times |\text{SetN} \times tL(I_q)|)) \quad (12)$$

The objective function is a method evaluation metric, while Idx is an index function that determines the position of the n-th node [95]. It informs the attacker, chaser,

barrier, and driver of each round's results. Fitness functions are now available for creating a suitable route across gateways and BS. Equation 13 specifies the distance in which gateways transit and Eq. 14 represents the gateway for the entire network [75].

$$D = \sum_{q=1}^Q \text{dst}(I_q, N \times tL(I_q)) \quad (13)$$

$$G_N = \sum_{p=1}^N NxtL \times \text{Count}(I_p) \quad (14)$$

It has been determined that the smallest number of hops would be utilized to route data, so the optimal route has been taken. Therefore, the objective function score for the result is positively correlated with the total distance covered and negatively correlated with the number of hops required to reach the destination [96]. The chimpanzee with the highest fitness level represents the ideal member of the population (attacker). Equation 15 is used to formulate the fitness function.

$$\text{Routing} - \text{Fitness} = \frac{\theta}{(\lambda_1 \times D + \lambda_2 \times G_N)}, \quad \lambda_1, \lambda_2 \in [0, 1], \lambda_1 + \lambda_2 = 1, \theta : \text{Proportionality Constant} \quad (15)$$

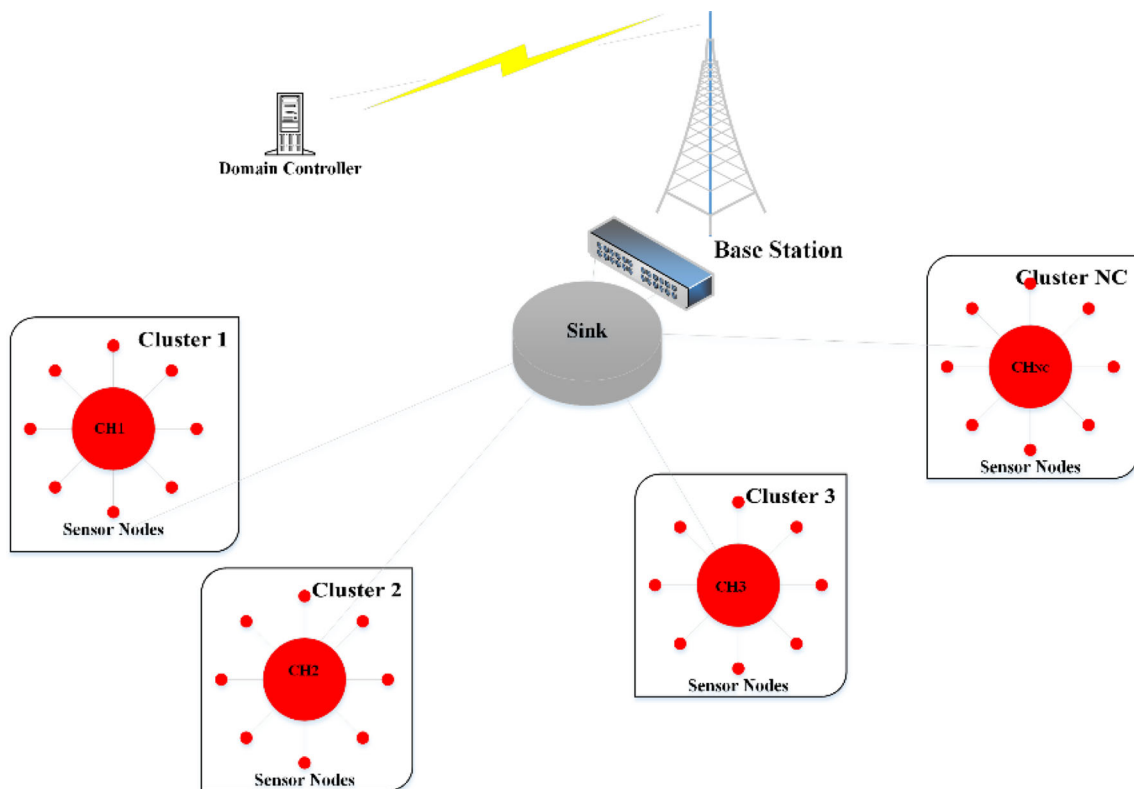


Fig. 2 Multi-hop clustering model in UWSNs

### 3.4.1 Fail-safe routing

The routing path may fail during the transmission of the data. This failure is because of various constraints like energy depletion at the nodes, and nodes movement from the cluster. It is essential to design the routing procedure to handle this worst-case scenario and continue the routing in alternate paths. The proposed procedure is modified so that the BS maintains the routing-fitness value based on Eq. 15 for all the possible routes found. The route with the highest fitness function is selected for routing initially. During the routing, the gateway maintains the number of packets transferred, and if the number of packets transferred within a particular period or energy utilized to transfer the packets exceeds the threshold, the second route with the highest fitness function will be used for transfer the rest of the packets until the first route is recovered from the workload. This condition is repeated until the best fitness route is recovered for further packet transfer. The modified routing procedure for fail-safe routing is provided in Table 3.

The modified routing procedure confirms the fail-safe operation by counting the number of packets transferred within a particular time, and also it considers the energy depletion that occurs at the gateway due to packet transfer. The selected route will only be used for packet transfer until the conditions are satisfied; the following route with a higher fitness value will be used for packet transfer. This modified procedure implements the fail-safe operation and load balancing and considers the gateway packets. For example, if the number of packets transferred through the gateway is more, it is overloaded. In this scenario, the procedure leads to the selection of the following higher fitness value route for packet routing, which eventually reduces the load in the gateway resulting in the prolonged

**Table 3** Fai-safe routing procedure

Start
Input: $\forall$ Route (R1, R2,...,Rn), PC- > packet count; RE- > Residual Energy(G); PCt- > packet count threshold; Ret- > residual energy threshold;
Output: Optimized Route (Rx) for routing
Select Rx = R1;
AA: Do
Route the packets through Route (Rx)
Increment PC
Decrement RE
While (PC < PCt && RE > REt)
Select Rx = following route with higher route fitness value;
Goto AA;

lifetime of the network. Thus the modified routing procedure achieves fail-safe operation and load balancing.

## 4 Experimentation and discussion

The effectiveness of HChOA is evaluated using the metrics listed below:

The energy utilization of each node during a given time is calculated using energy efficiency. The UWSN's total number of fully operational nodes is defined by two round numbers: Both the Final Node Count (FND) and the Half-Lifetime Node Count (HND) are rounded numbers that indicate when the network's central node and 50% of its nodes will die, respectively.

### 4.1 Implementation setup

The HChOA method is evaluated by simulating the UWSN in different situations based on the position of the BS, using a sequence implementation [97]. Figure 3 depicts three hypothetical situations labeled T1, T2, and T3, which describe the following: T1 indicates that the BS is in the middle of the target region; T2 indicates that BS is at one of the target region's corners, and T3 indicates that it is far from the targeted area. A hypothetical  $200 \times 200 \text{ m}^2$  area containing 300 nodes is considered. The parameters acquired for the process of validating are tabulated in Table 4. Three clustering approaches are used for comparison purposes: LEACH [98], TEEN [99], PSO [100], and IPSO-GWO [75].

### 4.2 Energy efficiency

As shown in Figs. 4, 5, 6, the efficiency of the resulting HChOA technique is validated by analyzing the maximum energy usage of three scenarios. Each sensor node's average energy retention over 2500 rotations is utilized to calculate how much energy is used.

Due to the inherent qualities of the chimp1 and chimp2 techniques for clustering and routing processes, HChOA provides a higher energy consumption than other models. The HChOA consumes the least energy possible when sending information through the cluster.

LEACH achieves an unsatisfactory outcome due to random CH selection and the utilization of one-hop communication. The energy used by the reactive TEEN approach is also lower than that of the LEACH process. However, it is inferior to the IPSO-GWO and HChOA algorithms. When compared to other models, the HChOA obtains a higher energy level. Since TEEN transmits data in all circumstances, it significantly minimizes the cost of communication. Since its random CH selection process,

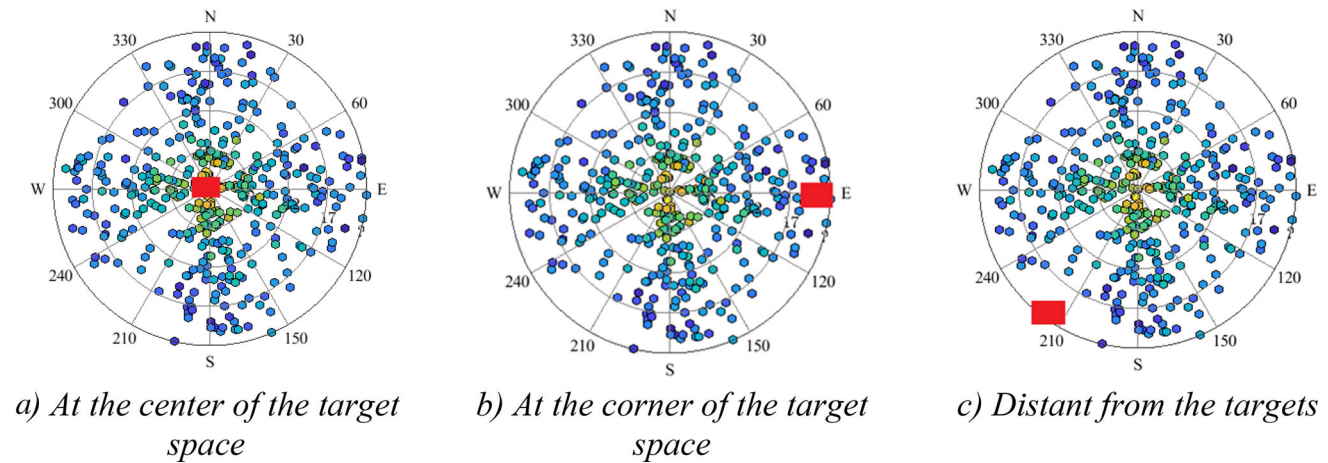


**Fig. 3** The BS's position

TEEN falls behind IPSO-GWO and HChOA in performance. IPSO-GWO employs a reliable approach for choosing CHs; nevertheless, the initial CHs are chosen at random.

### 4.3 The quantity of data transmission

Productive data transmissions between CHs and BSs during a certain time are typically used to measure a UWSN's efficacy. Until HND is reached, data aggregation conducted by CHs will be beneficial. Due to its effective routing method and disjointed clustering procedure, the HChOA model significantly increases the HND. Figure 7 shows how many data transfers are associated with the different types of networks.

Compared to other models, the HChOA transmits a considerable volume of data. Additionally, LEACH transmits fewer frames per scene than other approaches. As a result, it is unable to control the CH and limit node-to-base station interaction. Concurrently, the TEEN only sends data packets when an event occurs.

The HChOA method outperforms competing approaches because it is able to disseminate information more often over a longer period. There are a variety of options for defining the lifespan of a network. Because neighboring nodes lead to identical information, the FND has little effect on the functioning of the network beyond a slight

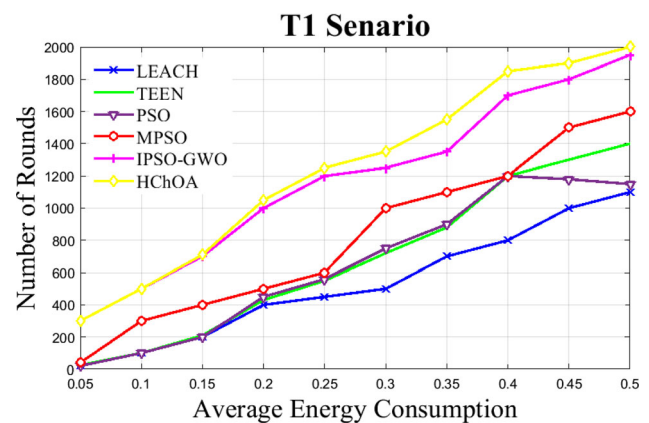


**Fig. 4**  $T_1$  Scenario

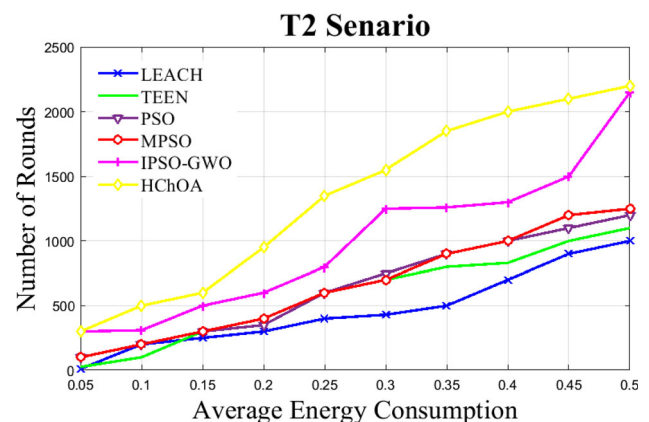


**Fig. 5**  $T_2$  Scenario

**Table 4** Setting parameters

Parameters	Value
Area	$200 \times 200 \text{ (m}^2\text{)}$
$E_0$	0.5 (J)
$E_{\text{elec}}$	500 (nJ/bit)
$\varepsilon_{fs}$	100 (pJ/bit/m <sup>2</sup> )
Packet size	4 (Kbits)

decrease in quality. The data quality is drastically reduced whenever an HND is earned at UWSN. If a node in a UWSN fails, the network as a whole stops doing anything, and the final node in the network stops talking to the base station. For the purpose of calculating the estimated remaining useful life of the network, both the FND and

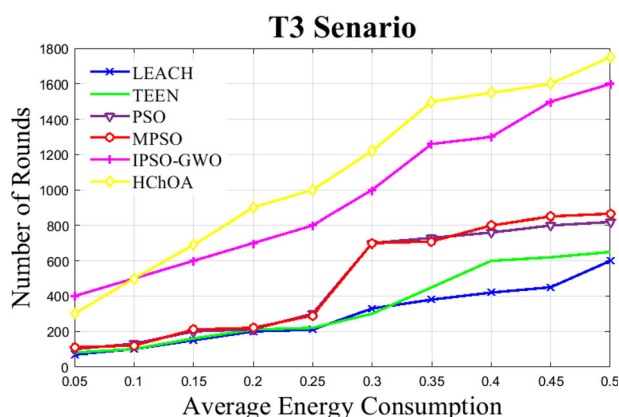


Fig. 6  $T_3$  scenario

HND measurements are taken into account. Results for the three scenarios in terms of FND and HND are displayed in Table 5 and Figs. 8 and 9.

Figure 8 demonstrates how the HChOA model outperforms alternative strategies in the first scenario. In the first case, the LEACH reaches FND at 799 rounds, whereas the HChOA arrives at 2133. In the second scenario, the LEACH experiences FND at 539 rounds and HChOA at 1875. In the third scenario, the HChOA experiences FND at 1633 rounds and LEACH at 460. The primary way in which the HChOA method lengthens the lifespan of the network is through the attainment of efficient energy usage.

Figure 9 shows that HChOA performs better than the other methods in the first case. Assuming Scenario 1, HND for LEACH happens at 1125, whereas HChOA arrives at 2145 rounds. In the second scenario, the LEACH reaches HND at 850 and HChOA at 2010. For the third scenario, the HChOA's HND happens at 1924 rounds and the LEACH at 615. Due to its improved energy efficiency, the HChOA model prolonged the network's lifespan.

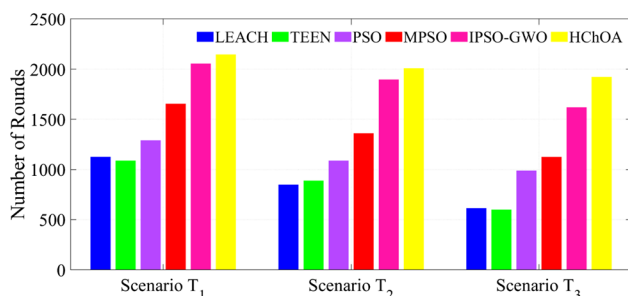


Fig. 7 Quantity of packets sent to BS prior to HND

#### 4.4 Computational complexity of hierarchical ChOA

The computational complexity of hierarchical ChOA depends on three variables: the total number of chimpanzees ( $n$ ), the maximum iterations required (MaxIter), and the sorting method used in each iteration. Due to their use of the rapid sorting approach, the complexity of these strategies is between  $O(n \times \log(n))$  and  $O(t \times n^2)$ . Equations (16) and (17) calculate the computational complexity of these methods.

$$O(\text{Hunting} - \text{Based}) = O(\text{MaxIter} \times (O(\text{position update}) + O(\text{Quick sort}))) \quad (16)$$

$$\begin{aligned} O(\text{Hunting} - \text{Based}) &= O((n \times d + n^2) \times \text{MaxIter}) \\ &= O(\text{MaxIter} \times d \times n + \text{MaxIter} \times n^2) \end{aligned} \quad (17)$$

#### 4.5 Statistical analysis of HChOA

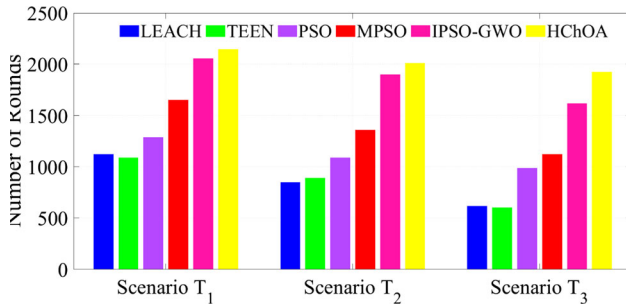
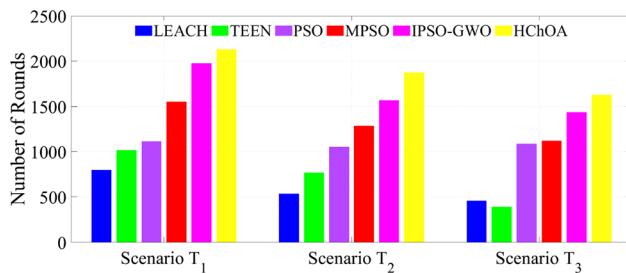
Bonferroni-Dunns, Friedman, and Holm tests compare HChOA to its pair competitors in this section. For an accurate evaluation, we used three different test scenarios. The examples are created to test the algorithms' abilities to avoid local minima and explore and utilize these minima when they occur. A comparison of the HChOA's performance with other benchmark algorithms is shown in Table 5. In terms of network lifespan results, HChOA outperformed all other algorithms. These results show that the well-tuned HChOA can transition between exploitative and exploratory phases and represents an outstanding performance to avoid local optima due to its hierarchical topology. The total rank of the benchmark algorithms is shown in Table 6 using Friedman's mean rank test. Table 6 shows that HChOA outperformed the other algorithms in the comparison.

A simple non-parametric Friedman test found a statistically significant difference in the algorithms' efficiency [101]. After displaying significant variances among various algorithms, it is necessary to establish whether the algorithms' performance differs significantly from HChOA [101]. We used a Bonferroni-Dunn post hoc test to compare pair-wise scores to establish statistical significance.

It is important to note that HChOA is used as the control approach in this test. Figure 10 shows the average ranking of each approach in the three situations with two degrees of significance of 0.1 and 0.05. HChOA can effectively outperform algorithms with a ranking average over the threshold line depicted in the figure. Every threshold line is

**Table 5** The results of network lifetime

Algorithms		LEACH	TEEN	PSO	MPSO	IPSO-GWO	HChOA
Scenario $T_1$	<i>FND</i>	799	1019	1115	1555	1979	2133
	<i>HND</i>	1125	1090	1290	1655	2057	2145
Scenario $T_2$	<i>FND</i>	539	770	1055	1290	1570	1875
	<i>HND</i>	850	890	1090	1360	1898	2010
Scenario $T_3$	<i>FND</i>	460	391	1089	1125	1440	1633
	<i>HND</i>	615	600	990	1124	1619	1924

**Fig. 8** FND for  $T_1$ ,  $T_2$  and  $T_3$  scenarios**Fig. 9** HND for  $T_1$ ,  $T_2$  and  $T_3$  scenarios

marked with a distinct color. The significance levels of 0.1 and 0.05 show that HChOA is ranked top across all classes and could significantly outperform LEACH, TEEN, PSO, MPSO, and IPSO-GWO.

Figure 10 shows that HChOA is more resilient and confident than high-performance optimizers when solving the given scenarios. The consistency of HChOA's performance across all three scenarios is evidenced by the slight variation in its average ranking. The rankings of other techniques, on the other hand, are inconsistent.

**Table 6** The result of the Friedman mean rank test

Algorithm	LEACH	TEEN	PSO	MPSO	IPSO-GWO	HChOA
Friedman mean rank	6.29	5.47	4.01	3.12	2.54	2.42
Rank	8	5	4	3	2	1

#### 4.6 Sensitivity analysis of designed model

This subsection investigates the sensitivity of three HChOA control parameters. Gauss-mouse, Sine-Bernoulli-Tent, and Bernoulli-Sine are chaotic maps, and their corresponding parameters  $\mathbf{m}$  and  $\mathbf{a}$  determine whether the chimps' position decreases or increases. The third parameter,  $\mu$ , determines whether regular position updates or updates based on chaotic maps are used. Based on the investigation results, it is clear that some parameters are more resistant to input-level changes than others. The best configuration of control parameters is also suggested. The four levels of parameters employed in the investigations are detailed in Table 7. As a result, the orthogonal array in Table 8 displays numerous parameter combinations and the derived cost function for different experiments. Finally, Fig. 11 depicts the parameters' level patterns based on Table 8 data.

To summarize, as shown by the experiment results, HChOA is most effective when its parameters are set to  $\alpha = 0.5$ ,  $\mathbf{m} = \text{Gauss/mouse}$ , and  $\mu = 0.5$ . An interpretation of the results is that HChOA is more predisposed to exploration in the first few iterations of the Gauss/mouse map because of its high amplitude; however, this amplitude and oscillations are reduced as the number of iterations increases. The algorithm is less likely to abandon promising locations if there are fewer oscillations during the exploitation phase. According to these findings, the optimal compromise between exploration and exploitation can be attained by setting both parameters to 0.5.



**Fig. 10** Bonferroni–Dunn’s test for  $\alpha = 0.05$  and  $\alpha = 0.1$

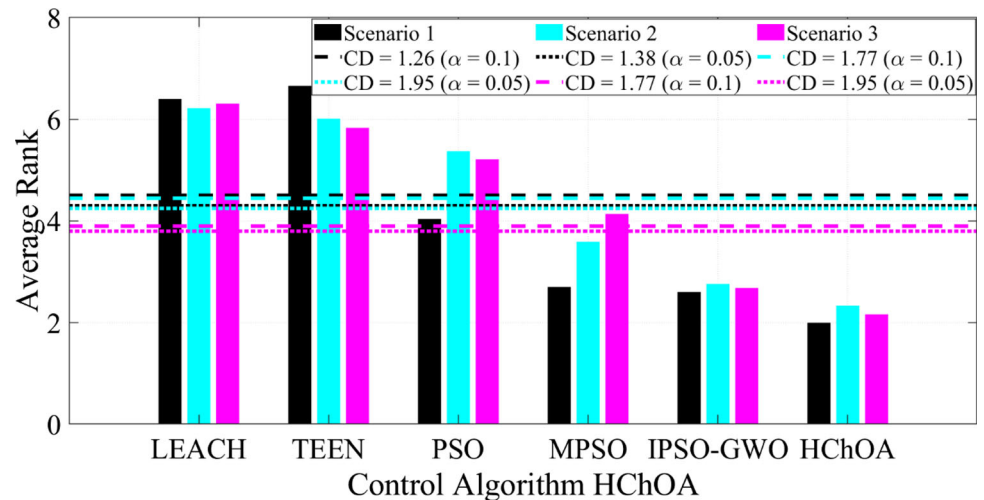


**Table 7** the specification of parameters

Parameters	Level			
	I	II	III	IV
<b>a</b>	0.2	0.5	0.8	1
<b>m</b>	Gauss/mouse	Sine	Tent	Bernoulli
<b><math>\mu</math></b>	0.2	0.5	0.8	1

**Table 8** Results of parameter combinations

Experiment number	The level of parameters			Cost function
	<b>a</b>	<b>m</b>	<b><math>\mu</math></b>	
				0.2185
1	I	I	I	0.0622
2	I	II	II	0.2676
3	I	III	III	0.1921
4	I	IV	IV	0.0010
5	II	I	II	0.2144
6	II	II	I	0.0120
7	II	III	IV	0.0048
8	II	IV	III	0.0900
9	III	I	I	0.0752
10	III	II	IV	0.0446
11	III	III	II	0.2871
12	III	IV	III	0.1472
13	IV	I	IV	0.1060
14	IV	II	III	0.1249
15	IV	III	II	0.1119
16	IV	IV	I	0.2185

## 4.7 Convergence analysis of HChOA

In this part, we examine HChOA’s experimental convergence. HChOA convergence is evaluated using measures

such as average fitness history, converging curve, and trajectories. Figure 12 depicts HChOA’s performance and convergence evaluation in three test scenarios.

In these cases, we can see a smooth progression of the convergence curve, showing that the findings are becoming better with each iteration. From each scenario, it can be seen that HChOA can begin with the best possible answer and refine it with each subsequent iteration.

The best chimp behavior for success can be shown in the convergence curve when chimps are viewed as community members. However, no data is available on the overall performance of the community. This is why the average fitness history metric measures community performance. This metric follows a similar pattern to the convergence curve but emphasizes how the group effort enhances the results of the original randomized population. The phase shift of the algorithm improves the fitness of all individuals. This improvement causes a step-like trend to emerge in the typical fitness record.

This figure’s third column shows the direction in which the agents are moving. This metric illustrates an agent’s topological shifts from its initial state to its final, optimized state. We used the first dimension of the agents’ trajectory because they move in so many directions. In the early iterations, these figures show high-frequency and high-amplitude changes that will become blurred in the last iterations. This pattern ensures that an algorithm eventually converges to a global minimum region by affirming exploration behavior in the early iterations and switching to local exploring behavior in the final iterations.

Finally, the search history is evaluated in the figure’s fourth column. Chaos maps’ dynamic activity enables HChOA to show a pattern of agents’ collective searching behavior. In test scenarios, the significant pattern’s feature aids in achieving the desired outcomes.

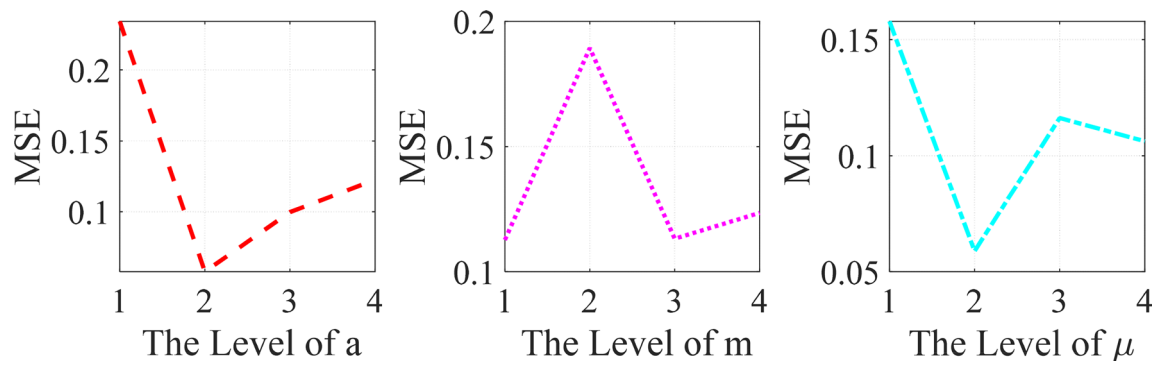


Fig. 11 Level trends of the analyzed parameters

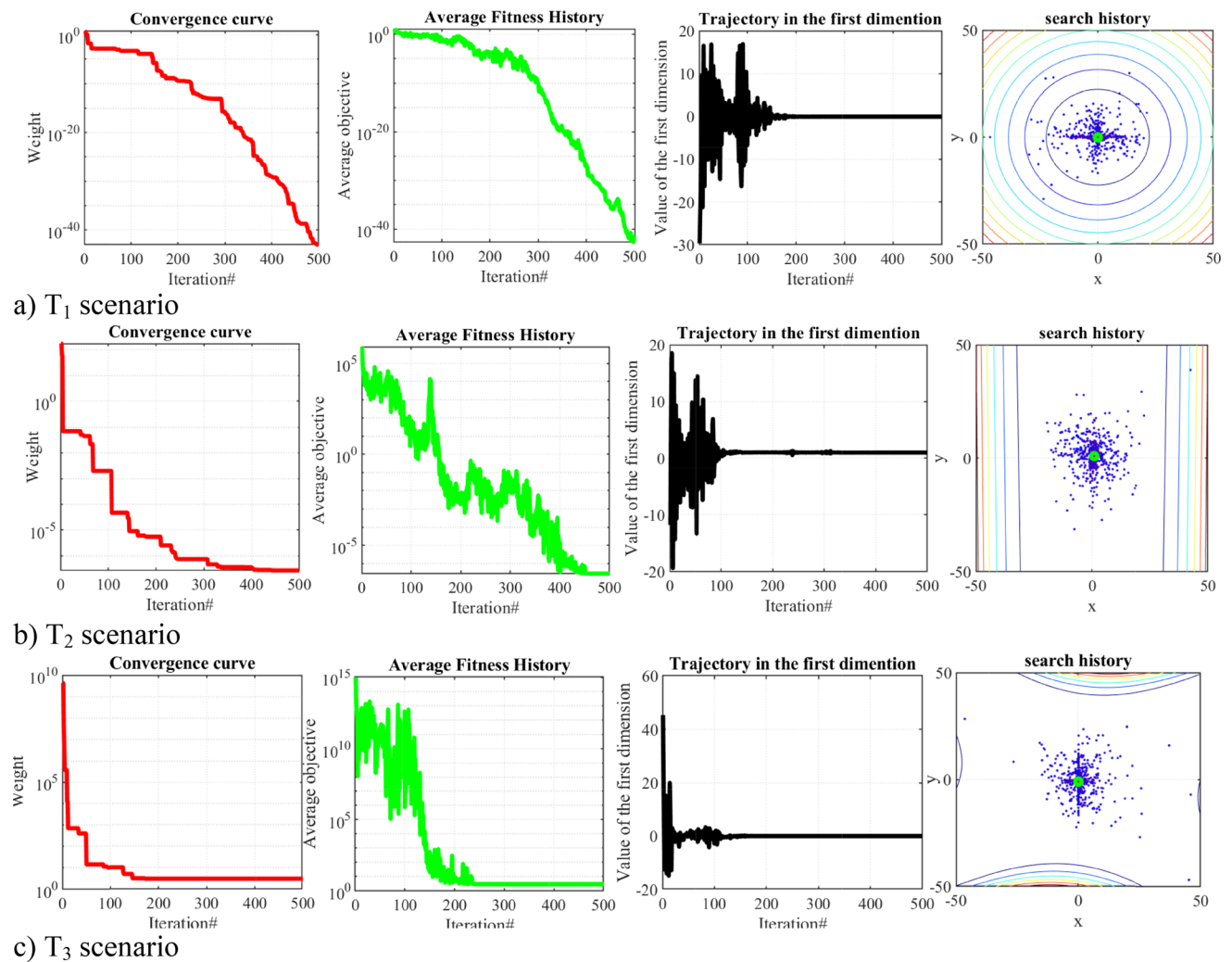


Fig. 12 Search history, average fitness history, convergence curve, and trajectory of three test scenarios. The first metric to show an optimal solution is the convergence curve

## 5 Conclusion

An HChOA-based clustering and multi-hop routing solution for UWSNs was detailed in this paper. We devised the HChOA method in this work, which has two primary

phases: chimp1 clustering and chimp2 routing. The CHs were selected using the chimp1 approach, which allowed for effective cluster organization. After that, the chimp2 routing process picks the most efficient routes across the system. As a result, the HChOA strategy suggested here

combines the best features of clustering and routing to maximize both energy consumption and network lifetime. Experimental analysis of the HChOA method was combined with evaluation parameters to confirm the simulation findings. The proposed HChOA method increased energy efficiency and the network's lifetime in simulations.

There are a variety of possible directions for further study. First, adaptive population sizes and co-evolutionary procedures are two ways to provide the suggested method with a more solid grounding in evolution. In addition, the computation can be executed in parallel using parallel computing techniques. Creating an HChOA variant with many objectives that can simultaneously be met is another promising line of inquiry.

**Data availability** Data sharing is not applicable to this article as no datasets were generated or analyzed during the current study.

## References

- Cheng, H., Shojafar, M., Alazab, M., Tafazolli, R., & Liu, Y. (2021). PPVF: Privacy-preserving protocol for vehicle feedback in cloud-assisted VANET. *IEEE Transactions on Intelligent Transportation Systems*, 23(7), 9391–9403.
- Cheng, B., Zhu, D., Zhao, S., & Chen, J. (2016). Situation-aware IoT service coordination using the event-driven SOA paradigm. *IEEE Transactions on Network and Service Management*, 13(2), 349–361.
- Jiang, Y., & Li, X. (2022). Broadband cancellation method in an adaptive co-site interference cancellation system. *International Journal of Electronics*, 109(5), 854–874.
- Yin, L., Wang, L., Keim, B. D., Konsoer, K., & Zheng, W. (2022). Wavelet analysis of dam injection and discharge in three gorges dam and reservoir with precipitation and river discharge. *Water*, 14(4), 567.
- Jiang, S., Zhao, C., Zhu, Y., Wang, C., & Du, Y. (2022). A practical and economical ultra-wideband base station placement approach for indoor autonomous driving systems. *Journal of Advanced Transportation*. <https://doi.org/10.1155/2022/3815306>
- Wang, K., Zhang, B., Alenezi, F., & Li, S. (2022). Communication-efficient surrogate quantile regression for non-randomly distributed system. *Information Sciences*, 588, 425–441.
- Zong, C., & Wang, H. (2022). An improved 3D point cloud instance segmentation method for overhead catenary height detection. *Computers & Electrical Engineering*, 98, 107685.
- Ren, Y., Jiang, H., Ji, N., & Yu, H. (2022). TBSM: A traffic burst-sensitive model for short-term prediction under special events. *Knowledge-Based Systems*, 240, 108120.
- Yan, L., Yin-He, S., Qian, Y., Zhi-Yu, S., Chun-Zi, W., & Zi-Yun, L. (2021). Method of reaching consensus on probability of food safety based on the integration of finite credible data on block chain. *IEEE Access*, 9, 123764–123776.
- Lv, Z., Chen, D., Feng, H., Zhu, H., & Lv, H. (2021). Digital twins in unmanned aerial vehicles for rapid medical resource delivery in epidemics. *IEEE Transactions on Intelligent Transportation Systems*, 23(12), 25106–25114.
- Chen, H., & Wang, Q. (2021). Regulatory mechanisms of lipid biosynthesis in microalgae. *Biological Reviews*, 96(5), 2373–2391.
- Li, D., Ge, S. S., & Lee, T. H. (2020). Fixed-time-synchronized consensus control of multiagent systems. *IEEE Transactions on Control of Network Systems*, 8(1), 89–98.
- Zhou, G., et al. (2021). An innovative echo detection system with STM32 gated and PMT adjustable gain for airborne LiDAR. *International Journal of Remote Sensing*, 42(24), 9187–9211.
- Zhou, G., et al. (2021). Gaussian inflection point selection for LiDAR hidden echo signal decomposition. *IEEE Geoscience and Remote Sensing Letters*, 19, 1–5.
- Zenggang, X., et al. (2022). Social similarity routing algorithm based on socially aware networks in the big data environment. *Journal of Signal Processing Systems*, 94(11), 1–15.
- Xiong, Z., et al. (2023). A comprehensive confirmation-based selfish node detection algorithm for socially aware networks. *Journal of Signal Processing Systems*. <https://doi.org/10.1007/s11265-023-01868-6>
- Chen, H., Miao, Y., Chen, Y., Fang, L., Zeng, L., & Shi, J. (2021). Intelligent model-based integrity assessment of nonstationary mechanical system. *Journal of Web Engineering*, 20(2), 253–280.
- Li, L., Wang, P., Zheng, X., Xie, Q., Tao, X., & Velásquez, J. D. (2023). Dual-interactive fusion for code-mixed deep representation learning in tag recommendation. *Information Fusion*, 99, 101862.
- Xie, X., Huang, L., Marson, S. M., & Wei, G. (2023). Emergency response process for sudden rainstorm and flooding: Scenario deduction and Bayesian network analysis using evidence theory and knowledge meta-theory. *Natural Hazards*. <https://doi.org/10.1007/s11069-023-05988-x>
- Xie, X., Tian, Y., & Wei, G. (2023). Deduction of sudden rainstorm scenarios: Integrating decision makers' emotions, dynamic Bayesian network and DS evidence theory. *Natural Hazards*, 116(3), 2935–2955.
- Wu, Z., Cao, J., Wang, Y., Wang, Y., Zhang, L., & Wu, J. (2018). hPSD: A hybrid PU-learning-based spammer detection model for product reviews. *IEEE Transactions on Cybernetics*, 50(4), 1595–1606.
- Zheng, W., Liu, X., & Yin, L. (2021). Research on image classification method based on improved multi-scale relational network. *PeerJ Computer Science*, 7, e613.
- Lv, Z., Chen, D., Feng, H., Wei, W., & Lv, H. (2022). Artificial intelligence in underwater digital twins sensor networks. *ACM Transactions on Sensor Networks*, 18(3), 1–27.
- Nguyen, N.-T., Le, T. T. T., Nguyen, H.-H., & Voznak, M. (2021). Energy-efficient clustering multi-hop routing protocol in a UWSN. *Sensors*, 21(2), 627.
- Cao, B., Zhao, J., Gu, Y., Fan, S., & Yang, P. (2019). Security-aware industrial wireless sensor network deployment optimization. *IEEE Transactions on Industrial Informatics*, 16(8), 5309–5316.
- Cao, B., et al. (2019). Multiobjective 3-D topology optimization of next-generation wireless data center network. *IEEE Transactions on Industrial Informatics*, 16(5), 3597–3605.
- Wang, X., & Lyu, X. (2021). Experimental study on vertical water entry of twin spheres side-by-side. *Ocean Engineering*, 221, 108508.
- Mou, J., Duan, P., Gao, L., Liu, X., & Li, J. (2022). An effective hybrid collaborative algorithm for energy-efficient distributed permutation flow-shop inverse scheduling. *Future Generation Computer Systems*, 128, 521–537.
- Yao, Y., Zhao, J., Li, Z., Cheng, X., & Wu, L. (2023). Jamming and eavesdropping defense scheme based on deep reinforcement

- learning in autonomous vehicle networks. *IEEE Transactions on Information Forensics and Security*, 18, 1211–1224.
30. Liu, G. (2023). A Q-learning-based distributed routing protocol for frequency-switchable magnetic induction-based wireless underground sensor networks. *Future Generation Computer Systems*, 139, 253–266.
  31. Xia, Y., Ding, L., & Tang, Z. (2023). Interaction effects of multiple input parameters on the integrity of safety instrumented systems with the k-out-of-n redundancy arrangement under uncertainties. *Quality and Reliability Engineering International*. <https://doi.org/10.1002/qre.3359>
  32. She, Q., Hu, R., Xu, J., Liu, M., Xu, K., & Huang, H. (2022). Learning high-DOF reaching-and-grasping via dynamic representation of gripper-object interaction. *arXiv Prepr. arXiv2204.13998*
  33. Xiao, Z., et al. (2021). Understanding private car aggregation effect via spatio-temporal analysis of trajectory data. *IEEE Transactions on Cybernetics*, 53(4), 2346–2357. <https://doi.org/10.1109/TCYB.2021.3117705>
  34. Jiang, H., Wang, M., Zhao, P., Xiao, Z., & Dustdar, S. (2021). A utility-aware general framework with quantifiable privacy preservation for destination prediction in LBSs. *IEEE/ACM Transactions on Networking*, 29(5), 2228–2241.
  35. Cao, K., et al. (2020). Improving physical layer security of uplink NOMA via energy harvesting jammers. *IEEE Transactions on Information Forensics and Security*, 16, 786–799.
  36. Cao, K., et al. (2021). Achieving reliable and secure communications in wireless-powered NOMA systems. *IEEE Transactions on Vehicular Technology*, 70(2), 1978–1983.
  37. Ma, K., et al. (2021). Reliability-constrained throughput optimization of industrial wireless sensor networks with energy harvesting relay. *IEEE Internet of Things Journal*, 8(17), 13343–13354.
  38. Chen, D., Li, Y., Li, X., Hong, X., Fan, X., & Savidge, T. (2022). Key difference between transition state stabilization and ground state destabilization: Increasing atomic charge densities before or during enzyme–substrate binding. *Chemical Science*, 13(27), 8193–8202.
  39. Yang, D., Zhu, T., Wang, S., Wang, S., & Xiong, Z. (2022). LFRSNet: A robust light field semantic segmentation network combining contextual and geometric features. *Frontiers in Environmental Science*, 10, 1443. <https://doi.org/10.3389/fenvs.2022.996513>
  40. Dai, B., Zhang, B., Niu, Z., Feng, Y., Liu, Y., & Fan, Y. (2022). A novel ultrawideband branch waveguide coupler with low amplitude imbalance. *IEEE Transactions on Microwave Theory and Techniques*, 70(8), 3838–3846.
  41. Li, J., Xu, K., Chaudhuri, S., Yumer, E., Zhang, H., & Guibas, L. (2017). Grass: Generative recursive autoencoders for shape structures. *ACM Transactions on Graphics*, 36(4), 1–14.
  42. Zhang, L., Zheng, H., Cai, G., Zhang, Z., Wang, X., & Koh, L. H. (2022). Power-frequency oscillation suppression algorithm for AC microgrid with multiple virtual synchronous generators based on fuzzy inference system. *IET Renewable Power Generation*, 16(8), 1589–1601.
  43. Mohajer, A., Sorouri, F., Mirzaei, A., Ziaeddini, A., Rad, K. J., & Bavaghar, M. (2022). Energy-aware hierarchical resource management and Backhaul traffic optimization in heterogeneous cellular networks. *IEEE Systems Journal*, 16(4), 5188–5199.
  44. Nikjoo, F., Mirzaei, A., & Mohajer, A. (2018). A novel approach to efficient resource allocation in NOMA heterogeneous networks: Multi-criteria green resource management. *Applied Artificial Intelligence*, 32(7–8), 583–612.
  45. Ma, Z., Zheng, W., Chen, X., & Yin, L. (2021). Joint embedding VQA model based on dynamic word vector. *PeerJ Computer Science*, 7, e353.
  46. Mohajer, A., Daliri, M. S., Mirzaei, A., Ziaeddini, A., Nabipour, M., & Bavaghar, M. (2022). Heterogeneous computational resource allocation for NOMA: Toward green mobile edge-computing systems. *IEEE Transactions on Services Computing*, 16(2), 1225–1238.
  47. Li, B., Zhang, M., Rong, Y., & Han, Z. (2021). Transceiver optimization for wireless powered time-division duplex MU-MIMO systems: Non-robust and robust designs. *IEEE Transactions on Wireless Communications*, 21(6), 4594–4607.
  48. Cheng, L., Yin, F., Theodoridis, S., Chatzis, S., & Chang, T.-H. (2022). Rethinking Bayesian learning for data analysis: The art of prior and inference in sparsity-aware modeling. *IEEE Signal Processing Magazine*, 39(6), 18–52.
  49. Zhou, G., Zhang, R., & Huang, S. (2021). Generalized buffering algorithm. *IEEE Access*, 9, 27140–27157.
  50. Li, B., Li, Q., Zeng, Y., Rong, Y., & Zhang, R. (2021). 3D trajectory optimization for energy-efficient UAV communication: A control design perspective. *IEEE Transactions on Wireless Communications*, 21(6), 4579–4593.
  51. Palan, N. G., Barbadekar, B. V., & Patil, S. (2017). Low energy adaptive clustering hierarchy (LEACH) protocol: A retrospective analysis. In *2017 International conference on inventive systems and control (ICISC)*, IEEE, pp. 1–12.
  52. Sandeep, D. N., & Kumar, V. (2017). Review on clustering, coverage and connectivity in underwater wireless sensor networks: A communication techniques perspective. *IEEE Access*, 5, 11176–11199.
  53. Zhu, F., & Wei, J. (2018). An energy efficient routing protocol based on layers and unequal clusters in underwater wireless sensor networks. *Journal of Sensors*, 2018, 1–10.
  54. Muruganathan, S. D., Ma, D. C. F., Bhasin, R. I., & Fapojuwo, A. O. (2005). A centralized energy-efficient routing protocol for wireless sensor networks. *IEEE Communications Magazine*, 43(3), S8–13.
  55. Durrani, M. Y., Tariq, R., Aadil, F., Maqsood, M., Nam, Y., & Muhammad, K. (2019). Adaptive node clustering technique for smart ocean under water sensor network (SOSNET). *Sensors*, 19(5), 1145.
  56. Khan, W., Wang, H., Anwar, M. S., Ayaz, M., Ahmad, S., & Ullah, I. (2019). A multi-layer cluster based energy efficient routing scheme for UWSNs. *IEEE Access*, 7, 77398–77410.
  57. Hong, Z., Pan, X., Chen, P., Su, X., Wang, N., & Lu, W. (2018). A topology control with energy balance in underwater wireless sensor networks for IoT-based application. *Sensors*, 18(7), 2306.
  58. Yu, W., Chen, Y., Wan, L., Zhang, X., Zhu, P., & Xu, X. (2020). An energy optimization clustering scheme for multi-hop underwater acoustic cooperative sensor networks. *IEEE Access*, 8, 89171–89184.
  59. Hou, R., He, L., Hu, S., & Luo, J. (2018). Energy-balanced unequal layering clustering in underwater acoustic sensor networks. *IEEE Access*, 6, 39685–39691.
  60. Baranidharan, V., Sivaradje, G., Varadharajan, K., & Vignesh, S. (2020). Clustered geographic-opportunistic routing protocol for underwater wireless sensor networks. *Journal of Applied Research and Technology*, 18(2), 62–68.
  61. Alqahtani, G. J., & Bouabdallah, F. (2021). Energy-efficient mobility prediction protocol for freely floating underwater acoustic sensor networks. *Frontiers in Communications and Networks*, 2, 692002.
  62. Mao, Y., Zhu, Y., Tang, Z., & Chen, Z. (2022). A novel airspace planning algorithm for cooperative target localization. *Electronics*, 11(18), 2950.
  63. Ahmadi, M., & Jameii, S. M. (2018). A secure routing algorithm for underwater wireless sensor networks. *International Journal of Engineering*, 31(10), 1659–1665.



64. Persis, D. J. (2019). A Bi-objective routing model for underwater wireless sensor network. In *Proceedings of the 2019 3rd international conference on intelligent systems, metaheuristics & swarm intelligence*, pp. 78–82.
65. Islam, T., & Park, S.-H. (2020). A two-stage routing protocol for partitioned underwater wireless sensor networks. *Symmetry (Basel)*, 12(5), 783.
66. Morsy, N. A., AbdelHay, E. H., & Kishk, S. S. (2018). Proposed energy efficient algorithm for clustering and routing in WSN. *Wireless Personal Communications*, 103(3), 2575–2598.
67. Lalwani, P., Das, S., Banka, H., & Kumar, C. (2018). CRHS: Clustering and routing in wireless sensor networks using harmony search algorithm. *Neural Computing and Applications*, 30(2), 639–659.
68. Lalwani, P., Banka, H., & Kumar, C. (2018). BERA: A bio-geography-based energy saving routing architecture for wireless sensor networks. *Soft Computing*, 22(5), 1651–1667.
69. Lalwani, P., Banka, H., & Kumar, C. (2017). CRWO: Clustering and routing in wireless sensor networks using optics inspired optimization. *Peer-to-Peer Networking and Applications*, 10(3), 453–471.
70. Mekonnen, M. T., & Rao, K. N. (2017). Cluster optimization based on metaheuristic algorithms in wireless sensor networks. *Wireless Personal Communications*, 97(2), 2633–2647.
71. Ezhilarasi, M., & Krishnaveni, V. (2019). An evolutionary multipath energy-efficient routing protocol (EMEER) for network lifetime enhancement in wireless sensor networks. *Soft Computing*, 23(18), 8367–8377.
72. Yogarajan, G., & Revathi, T. (2018). Improved cluster based data gathering using ant lion optimization in wireless sensor networks. *Wireless Personal Communications*, 98(3), 2711–2731.
73. Gao, F., Luo, W., & Ma, X. (2019). Energy constrained clustering routing method based on particle swarm optimization. *Cluster Computing*, 22(3), 7629–7635.
74. Sirdeshpande, N., & Udupi, V. (2017). Fractional lion optimization for cluster head-based routing protocol in wireless sensor network. *Journal of the Franklin Institute*, 354(11), 4457–4480.
75. Elhoseny, M., Rajan, R. S., Hammoudeh, M., Shankar, K., & Aldabbas, O. (2020). Swarm intelligence-based energy efficient clustering with multihop routing protocol for sustainable wireless sensor networks. *International Journal of Distributed Sensor Networks*, 16(9), 1550147720949133.
76. Zhang, X., Wang, Y., Yang, M., & Geng, G. (2021). Toward concurrent video multicast orchestration for caching-assisted mobile networks. *IEEE Transactions on Vehicular Technology*, 70(12), 13205–13220.
77. Wolpert, D. H., & Macready, W. G. (1997). No free lunch theorems for optimization. *IEEE Transactions on Evolutionary Computation*, 1(1), 67–82. <https://doi.org/10.1109/4235.585893>
78. Saffari, A., Khishe, M., & Zahiri, S.-H. (2022). “Fuzzy-ChOA: An improved chimp optimization algorithm for marine mammal classification using artificial neural network. *Analog Integrated Circuits and Signal Processing*, 111(3), 1–15. <https://doi.org/10.1007/s10470-022-02014-1>
79. Saffari, A., Zahiri, S. H., Khishe, M., & Mosavi, S. M. (2020). Design of a fuzzy model of control parameters of chimp algorithm optimization for automatic sonar targets recognition. *Iranian Journal of Marine Technology*, 9(1), 1–14.
80. Khishe, M., & Mosavi, M. R. (2020). Classification of underwater acoustical dataset using neural network trained by chimp optimization algorithm. *Applied Acoustics*. <https://doi.org/10.1016/j.apacoust.2019.107005>
81. Hu, T., Khishe, M., Mohammadi, M., Parvizi, G. R., Taher Karim, S. H., & Rashid, T. A. (2021). Real-time COVID-19 diagnosis from X-Ray images using deep CNN and extreme learning machines stabilized by chimp optimization algorithm. *Biomedical Signal Processing and Control*, 68, 102764. <https://doi.org/10.1016/j.bspc.2021.102764>
82. Houssein, E. H., Emam, M. M., & Ali, A. A. (2021). An efficient multilevel thresholding segmentation method for thermography breast cancer imaging based on improved chimp optimization algorithm. *Expert Systems with Applications*, 185, 115651. <https://doi.org/10.1016/j.eswa.2021.115651>
83. Wang, J., Khishe, M., Kaveh, M., & Mohammadi, H. (2021). Binary chimp optimization algorithm (BChOA): A new binary meta-heuristic for solving optimization problems. *Cognitive Computation*, 13(5), 1297–1316.
84. Gong, S.-P., Khishe, M., & Mohammadi, M. (2022). Niching chimp optimization for constraint multimodal engineering optimization problems. *Expert Systems with Applications*, 198, 116887.
85. Jabbar N. M. A., & Mitras, B. A. (2021). Modified chimp optimization algorithm based on classical conjugate gradient methods. In *Journal of Physics: Conference Series*, IOP Publishing, pp. 12027.
86. Liu, L., Khishe, M., Mohammadi, M., & Mohammed, A. H. (2022). Optimization of constraint engineering problems using robust universal learning chimp optimization. *Advanced Engineering Informatics*, 53, 101636.
87. Jia, H., Sun, K., Zhang, W., & Leng, X. (2021). An enhanced chimp optimization algorithm for continuous optimization domains. *Complex & Intelligent Systems*, 8, 1–18. <https://doi.org/10.1007/s40747-021-00346-5>
88. Khishe, M., Nezhadshahbodaghi, M., Mosavi, M. R., & Martín, D. (2021). A weighted chimp optimization algorithm. *IEEE Access*, 9, 158508–158539.
89. Kaidi, W., Khishe, M., & Mohammadi, M. (2021). Dynamic levy flight chimp optimization. *Knowledge-Based Systems*, 235, 107625.
90. Chen, F., Yang, C., & Khishe, M. (2022). Diagnose Parkinson’s disease and cleft lip and palate using deep convolutional neural networks evolved by IP-based chimp optimization algorithm. *Biomedical Signal Processing and Control*, 77, 103688.
91. Bo, Q., Cheng, W., Khishe, M., Mohammadi, M., & Mohammed, A. H. (2022). Solar photovoltaic model parameter identification using robust niching chimp optimization. *Solar Energy*, 239, 179–197.
92. Wu, J., Khishe, M., Mohammadi, M., Karim, S. H. T., & Shams, M. (2021). Acoustic detection and recognition of dolphins using swarm intelligence neural networks. *Applied Ocean Research*, 115, 102837.
93. Khishe, M., & Mosavi, M. R. (2020). Chimp optimization algorithm. *Expert Systems with Applications*. <https://doi.org/10.1016/j.eswa.2020.113338>
94. Liu, G. (2021). Data collection in mi-assisted wireless powered underground sensor networks: Directions, recent advances, and challenges. *IEEE Communications Magazine*, 59(4), 132–138.
95. Meng, F., Xiao, X., & Wang, J. (2022). Rating the crisis of online public opinion using a multi-level index system. arXiv Prepr. arXiv2207.14740
96. Cao, B., et al. (2021). Large-scale many-objective deployment optimization of edge servers. *IEEE Transactions on Intelligent Transportation Systems*, 22(6), 3841–3849.
97. Wang, S., Sheng, H., Yang, D., Zhang, Y., Wu, Y., & Wang, S. (2022). Extendable multiple nodes recurrent tracking framework with RTU++. *IEEE Transactions on Image Processing*, 31, 5257–5271.
98. Xiangning, F., & Yulin, S. (2007). Improvement on LEACH protocol of wireless sensor network. In *2007 International*



*conference on sensor technologies and applications (SENSORCOMM 2007)*, IEEE, pp. 260–264.

99. Manjeshwar, A., & Agrawal, D. P. (2001). TEEN: ARouting protocol for enhanced efficiency in wireless sensor networks. *Ipdps*, 1, 189.
100. Wu, X., Lei, S., Jin, W., Cho, J., & Lee, S. (2006) Energy-efficient deployment of mobile sensor networks by PSO. In *Asia-Pacific Web Conference*, Springer, pp. 373–382.
101. Wang, H., Gao, Q., Li, H., Wang, H., Yan, L., & Liu, G. (2022). A structural evolution-based anomaly detection method for generalized evolving social networks. *The Computer Journal*, 65(5), 1189–1199.

**Publisher's Note** Springer Nature remains neutral with regard to jurisdictional claims in published maps and institutional affiliations.

Springer Nature or its licensor (e.g. a society or other partner) holds exclusive rights to this article under a publishing agreement with the author(s) or other rightsholder(s); author self-archiving of the accepted manuscript version of this article is solely governed by the terms of such publishing agreement and applicable law.



**Shukun He** was born in Xinyi, Jiangsu P.R. China, in 1982. He graduated from Southwest Jiaotong University, P.R. China, with a bachelor's degree in computer science and technology. Now, He is a lecturer at Chongqing creation vocational college. His research interests include artificial intelligence, information security, Internet of Things and Big data analysis.



**Qinlin Li** was born in Neijiang, Sichuan, China, in 1986. He received his master's degree from Southwest Jiaotong University, Sichuan, China. He studies in Faculty of Engineering, Technology and Built Environment, UCSI University. His research interests include control theory, image processing and electronic information.



**Mohammad Khishe** received a B.Sc. degree in Maritime Electronics and Communication Engineering from Imam Khomeini Maritime Sciences University, Nowshahr, Iran in 2007 and also, M.Sc. and Ph. D. degrees in Electronic Engineering from Islamic Azad University, Qazvin branch, and Iran University of Science and Technology, Tehran in 2012 and 2017, respectively. Since 2017, he is an assistant professor at Imam Khomeini Maritime Sciences

University, Nowshahr, Iran. Currently, he is associate professor at Imam Khomeini Maritime Sciences University, Nowshahr, Iran. His research interests are Optimization, Artificial Neural Networks, Meta-heuristic Algorithms, Sonar and Radar Signal Processing, and FPGA design.

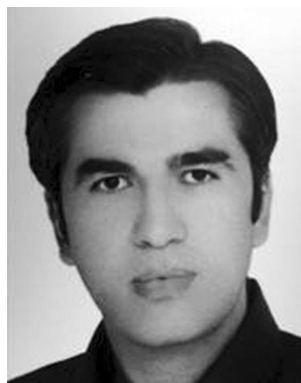


**Amin Salih Mohammed** currently serves as President of Lebanese French University, Erbil, Kurdistan region-Iraq. Before being promoted to President, he served as Vice President, Scientific Affairs of the university. He is an active IEEE Senior Member. He has more than 17 years of teaching and research experience. Amin is an active researcher and acted as a resource person for various workshops and faculty development programs organized by

multiple international institutions. As tech-savvy, He has completed his undergraduate, postgraduate engineering degree and Ph.D. in Computer Engineering from the Kharkiv National University of Radio Electronics, Kharkiv, Ukraine. His research fields are computer networks, wireless networks, and cloud computing. So far, he has published more than 50 research articles in various reputed international journals indexed in SCI & Scopus databases and reputed international IEEE conferences.



**Hassan Mohammadi** was born on March 21, 1981 in Razavi Khorasan province in Iran. He is currently a PhD student in Electrical-Electronic Engineering at the Islamic Azad University, Sari branch. His areas of interest are solar wind hybrid systems, power electronics, power quality and microgrids. He is currently one of the senior managers of Mazandaran Science and Technology Park.



**Mokhtar Mohammadi** received the B.S. degree in computer engineering from Shahed University, Tehran, Iran, in 2003, the M.S. degree in computer engineering from Shahid Beheshti University, Tehran, Iran, in 2012, and the Ph.D. degree in computer engineering from Shahrood University of Technology, Shahrood, Iran, in 2018. His current research interests include signal processing, time-frequency analysis, and machine learning. He is

currently with the Department of Information Technology, Lebanese French University-Erbil, Iraq.

## Authors and Affiliations

Shukun He<sup>1</sup> · Qinlin Li<sup>2,3</sup> · Mohammad Khishe<sup>4</sup>  · Amin Salih Mohammed<sup>5,6</sup> · Hassan Mohammadi<sup>4</sup> · Mokhtar Mohammadi<sup>7</sup>

✉ Mohammad Khishe  
m\_khishe@alumni.iust.ac.ir

✉ Amin Salih Mohammed  
amin.mohammed@su.edu.krd

Shukun He  
heshukun1982@126.com

Qinlin Li  
liqinlin@cduetec.edu.cn

Mokhtar Mohammadi  
Mokhtar@lfu.edu.krd

<sup>3</sup> Department of Electrical and Electronics Engineering, Faculty of Engineering, Technology and Built Environment, UCSI University, Cheras 56000, Kuala Lumpur, Malaysia

<sup>4</sup> Department of Electrical Engineering, Imam Khomeini Marine Science University, Nowshahr, Iran

<sup>5</sup> Department of Software and Informatics Engineering, College of Engineering, Salahaddin University, Erbil, Kurdistan Region, Iran

<sup>6</sup> Department of Computer Engineering, College of Engineering and Computer Science, Lebanese French University, Erbil, Kurdistan Region, Iraq

<sup>7</sup> Department of Information Technology, College of Engineering and Computer Science, Lebanese French University, Erbil, Kurdistan Region, Iraq

<sup>1</sup> School of Artificial Intelligence, Chongqing Creation Vocational College, Yongchuan, Chongqing 402160, China

<sup>2</sup> Faculty of Engineering, Chengdu College of University of Electronic Science and Technology of China, Chengdu 611731, Sichuan, China